PROCEEDINGS OF SCIENCE

Higgs self-coupling measurements at the FCC-hh

Birgit Stapf,[a,*] **Angela Taliercio,**[c] **Elisabetta Gallo,**[a,b] **Kerstin Tackmann**[a,b] **and Paola Mastrapasqua**[d]

[a] *Institut für Experimentalphysik, Universität Hamburg, Luruper Chaussee 149, 22761 Hamburg, Germany*

[b] *Deutsches Elektronen-Synchrotron DESY Notkestr. 85, 22607 Hamburg, Germany*

[c] *Northwestern University, Evanston, Illinois, USA*

[d] *Centre for Cosmology, Particle Physics and Phenomenology (CP3), Université catholique de Louvain, Louvain-la-Neuve, Belgium*

E-mail: birgit.stapf@desy.de

The hadron collider phase of the Future Circular Collider (FCC-hh) is a proton-proton collider operating at a center-of-mass energy of 100 TeV. It is one of the most ambitious projects planned for the rest of this century and offers ample opportunities in the hunt for new physics, both through its direct detection reach as well as through indirect evidence from precision measurements. Extracting a precision measurement of the Higgs self-coupling from the Higgs pair production cross-section will play a key role in our understanding of electroweak symmetry breaking, as the self-coupling gives insight into the nature of the Higgs potential. With the large data set of in total 30 ab^{-1} which is envisioned to be collected during the FCC-hh runtime the Higgs self-coupling will be determined down to the percent level. This paper presents prospect studies for Higgs self-coupling measurements in the $b\bar{b}\gamma\gamma$ and $b\bar{b}\ell\ell + E_{\mathrm{T}}^{\mathrm{miss}}$ final states, with the combined, expected precision on the Higgs self-coupling modifier κ_λ reaching 3.2-5.7% at 68% confidence level, assuming all other Higgs couplings follow their Standard Model expectations and depending on the systematic uncertainties assumed. This high precision is mostly driven by the $b\bar{b}\gamma\gamma$ final state analysis, while the $b\bar{b}\ell\ell + E_{\mathrm{T}}^{\mathrm{miss}}$ final state - newly studied for its FCC-hh prospects in this document - on its own reaches a maximum precision of roughly 20% on κ_λ.

The European Physical Society Conference on High Energy Physic (EPS-HEP 2023)
21-25 August 2023
Hamburg, Germany

*Speaker

PoS(EPS-HEP2023)413

1. Introduction

The study of Higgs boson pair production is one of the key benchmarks of the scientific program at future colliders. It offers direct experimental access to the Higgs boson trilinear self-coupling and hence to the structure of the scalar potential itself, allowing unprecedented insight into the electroweak symmetry breaking mechanism. The self-coupling modifier κ_λ, defined as the ratio of the measured value of the self-coupling over its Standard Model (SM) predicted value - λ/λ_{SM} - is used to parameterise any deviation from the SM expectations. A precision measurement of κ_λ down to the percent level is a clear goal for future experiments, as at the end of the HL-LHC era the κ_λ precision is expected to reach only around 50% [1]. The envisioned proton-proton collision phase of the Future Circular Collider (FCC-hh) would provide a total data set of 30 ab^{-1}, at a centre-of-mass energy of $\sqrt{s}$= 100 TeV [2], making a precision measurement of κ_λ possible.
In this document, we present an updated strategy for the analysis of the $b\bar{b}\gamma\gamma$ final state with respect to previous self-coupling studies at FCC-hh [3], as well as a new study for FCC-hh using $b\bar{b}\ell\ell + E_{\mathrm{T}}^{\mathrm{miss}}$ final state events.

2. Event generation, detector simulation and data analysis

Proton-proton collision events at $\sqrt{s}$= 100 TeV using a fast detector simulation with the DELPHES framework [4] form the basis of the prospect studies. The signals, constituted by gluon-gluon fusion induced double Higgs production events for different values of κ_λ, are generated with POWHEG [5–7] at next-to-leading order (NLO). The respective cross-sections are scaled to NNLO using a k-factor that is independent of κ_λ [8] (following [3] and motivated by the studies in [9]). All background processes are generated with MADGRAPH5_aMC@NLO [10, 11]. For all samples, the hadronisation effects as well as the Higgs decays are modeled with PYTHIA 8 [12]. An optimistic, nearly ideal detector is assumed, with identification efficiencies reaching above 90% and momentum resolutions in the per mille range, parameterised in terms of the kinematic properties of each object.
It is important to highlight that the technical implementation of all the above steps is part of the KEY4HEP project [13], that provides a consistent software stack for *all* future collider facilities. In particular, the samples used here are in EDM4HEP format [14]. These samples are processed with the FCCANALYSES framework [15].

2.1 $b\bar{b}\gamma\gamma$ analysis

Although the $b\bar{b}\gamma\gamma$ final state is rare, with a branching ratio of 0.26%, it provides excellent sensitivity on κ_λ due to its clean signature with well-reconstructed objects, namely two photons and two b-jets. The full HH system can be reconstructed with good resolution. Backgrounds arise from single Higgs events and the non-resonant QCD-induced production of two isolated, energetic photons.
To maximize the sensitivity, a multi-variate analysis strategy is employed, relying on different Deep Neural Networks (DNN) to suppress the different backgrounds. The DNNs are implemented using a Keras frontend [16] with a tensorflow backend [17]. Figure 1a summarizes the various steps of the analysis strategy. First, a DNN is trained to differentiate between the signals and the $t\bar{t}H$ background. The contribution of the $t\bar{t}H$ background is enhanced among the single Higgs production modes since it results in a similar final state as the signal. However, its characteristic

kinematics differ from those of the signal: generally, $t\bar{t}H$ events have more, but less energetic jets and/or leptons with large transverse momentum, and in the signal the photon and b-jet pair are expected to be back-to-back, so with a large angle between them, but small angles within each pair. All of this information is exploited by the DNN based $t\bar{t}H$-tagger. As can be seen in Figure 1b showing the DNN scores, the tagger provides good separation between signal and the targeted $t\bar{t}H$ background. For the next step, events are divided into two categories based on the invariant mass $m_X = m_{b\bar{b}\gamma\gamma} - m_{b\bar{b}} - m_{\gamma\gamma} + 250\,\text{GeV}$, which reconstructs the di-Higgs mass corrected for resolution effects. As illustrated in Figure 1c, the shape of this distribution depends on κ_λ. Two separate DNNs, with the same setup and input variables as the $t\bar{t}H$ tagger are trained to discriminate the signals from the remaining backgrounds. Figure 1d shows the resulting scores for the example of events with $m_X > 350$ GeV. A multi-dimensional optimization procedure with the significance as the figure of merit is performed to 1) discard events below a lower threshold on the DNN scores and 2) define a medium and high purity region based on the score of the second DNN. Last, events are categorized into a central or sideband region according to the value of the invariant mass of the b-jet pair, m_{bb}, using a window around the Higgs mass of around 15 GeV. This full procedure results in eight categories, in which the invariant diphoton mass $m_{\gamma\gamma}$ is used in the likelihood fit to extract κ_λ. Figure 1e shows the $m_{\gamma\gamma}$ distributions in an example central region.

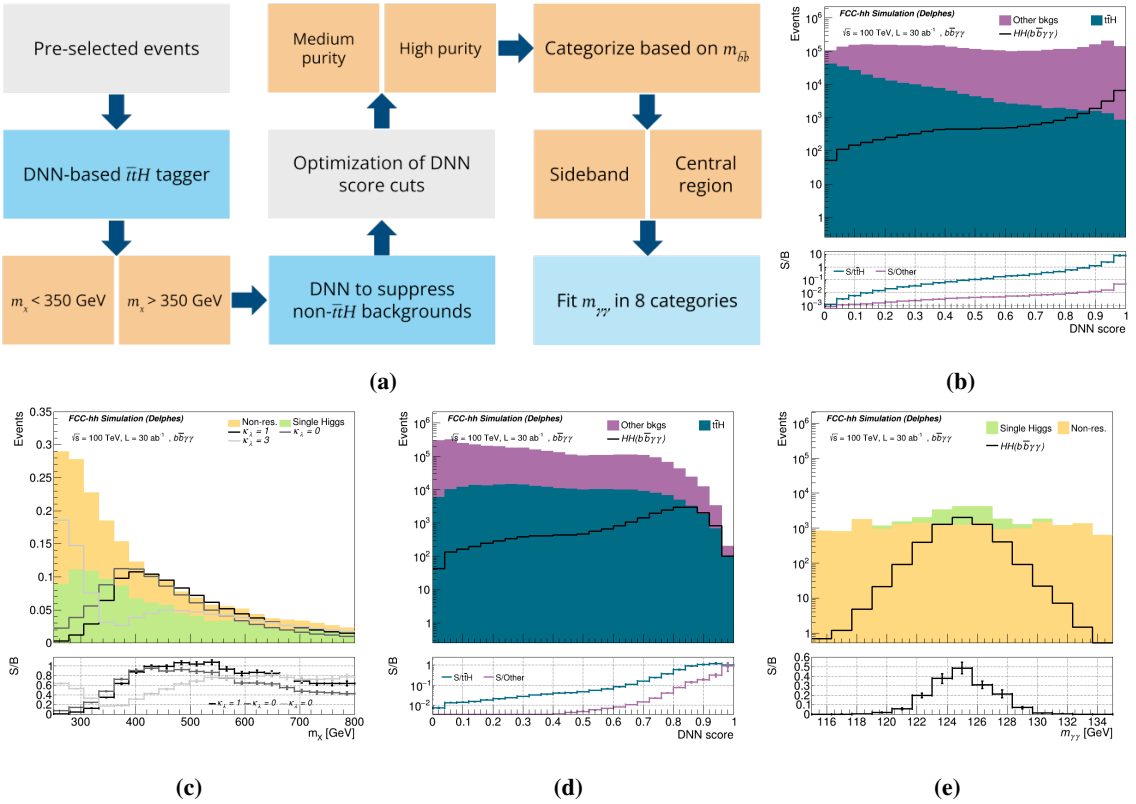

Figure 1: a) Overview of the $b\bar{b}\gamma\gamma$ analysis strategy. b) Distributions of the DNN score of the $t\bar{t}H$ tagger. c) Distributions of the reconstructed m_X for different anomalous coupling hypotheses and the background. d) Distributions of the DNN score to suppress non-$t\bar{t}H$ backgrounds, for events with $m_X > 350$ GeV. And e) distributions of the invariant mass $m_{\gamma\gamma}$ in an example central region.

2.2 $b\bar{b}\ell\ell + E_{\mathrm{T}}^{\mathrm{miss}}$ analysis

The $b\bar{b}\ell\ell + E_{\mathrm{T}}^{\mathrm{miss}}$ analysis considers the sum of signals from the $HH \to b\bar{b}WW^* \to b\bar{b}\ell\nu\ell\nu$, $HH \to b\bar{b}\tau\tau \to b\bar{b}\ell\nu\ell\nu$ and $HH \to b\bar{b}ZZ^* \to b\bar{b}\ell\ell\nu\nu$ Higgs pair decays. Together, their branching ratio amounts to 3.24%, so these type of events are an order of magnitude more common than $b\bar{b}\gamma\gamma$ events. Nonetheless, the $b\bar{b}\ell\ell + E_{\mathrm{T}}^{\mathrm{miss}}$ analysis is more difficult. The final state involves missing transverse energy $E_{\mathrm{T}}^{\mathrm{miss}}$ from neutrinos escaping detection, so reconstructing one of the two Higgs decays fully is not possible. Moreover, the dileptonic decay of a top quark pair leads to the same the final state: two b-jets, two charged light leptons (electrons or muons) and $E_{\mathrm{T}}^{\mathrm{miss}}$. The production cross-section of this irreducible $t\bar{t}$ background is seven orders of magnitude larger than that of the $b\bar{b}\ell\ell + E_{\mathrm{T}}^{\mathrm{miss}}$ signal. Additional backgrounds arise from single Higgs and single top production, the V + jets Drell-Yan process and the production of a top quark pair together with vector boson(s).

A cut-based analysis is implemented to enhance sensitivity, exploiting the expected signal kinematics sketched in Figure 2a. In particular, the overwhelmingly large $t\bar{t}$ background can be efficiently suppressed employing a lower bound on the minimum average invariant mass of the lepton and b-jet pairs, $m_{\ell b}^{\mathrm{reco}} = \min\left(\frac{m_{\ell_1 b_1}+m_{\ell_2 b_2}}{2}, \frac{m_{\ell_2 b_1}+m_{\ell_1 b_2}}{2}\right)$, which is used in measurements of the top quark mass [18]. Figure 2b shows the distributions of this variable in signal and background. To capture the full HH decay, the *stransverse mass* m_{T2} [19] which predicts the invisible mass contribution from the neutrinos is used in the likelihood fit in this channel. This is done in five categories based on the flavours of the leptons, whether a resonant Z-decay is present and the angle between the leptons and $E_{\mathrm{T}}^{\mathrm{miss}}$. Figure 2c shows the m_{T2} distributions in an example category.

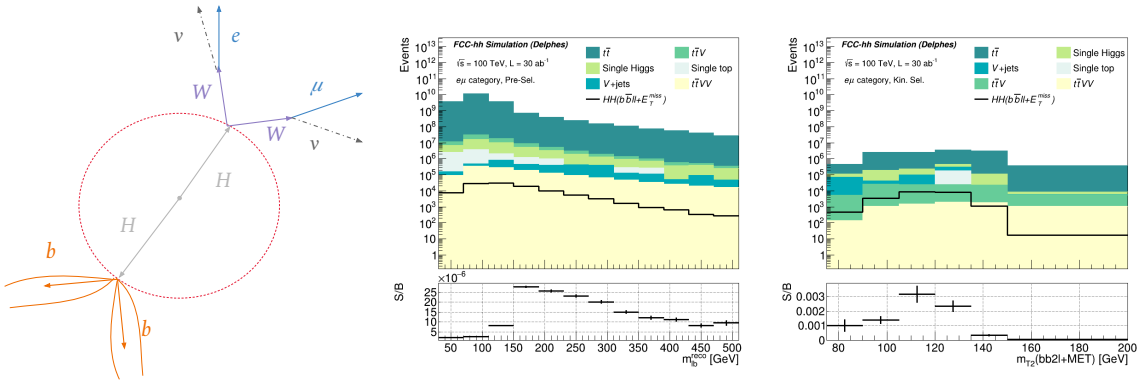

(a) **(b)** **(c)**

Figure 2: a) Sketch of (idealized) $HH \to b\bar{b}WW^* \to b\bar{b}\ell\nu\ell\nu$ event kinematics. b) Distributions of the $m_{\ell b}^{\mathrm{reco}}$ variable in events with an electron muon pair and two b-jets. And c) distributions of the stransverse mass m_{T2} after full kinematic selection, in the electron-muon category.

3. Results

The determination of the Higgs self-coupling modifier κ_λ is performed for three different scenarios of assumed systematic uncertainties, as listed in Table 1. Generally the systematic scenarios considered are optimistic (and in line with previous FCC-hh studies [3]), assuming for example that

for the $b\bar{b}\ell\ell + E_{\mathrm{T}}^{\mathrm{miss}}$ analysis the large $t\bar{t}$ and V + jets backgrounds will be measured in data control regions with high precision. The uncertainties are only considered as impact on the event rates, not on the kinematic distributions of the process they apply to.

	Source of uncertainty	Syst. 1	Syst. 2	Syst. 3	Applies to
Common	b-jet ID per b-jet	0.5%	1%	2%	Signals, MC bkgs.
	Luminosity	0.5%	1%	2%	Signals, MC bkgs.
	Signal cross-section	0.5%	1%	1.5%	Signals, MC bkgs.
$b\bar{b}\gamma\gamma$	γ ID per γ	0.5%	1%	2%	Signals, MC bkgs.
$b\bar{b}\ell\ell + E_T^{miss}$	Lepton ID per lepton	0.5%	1%	2%	Signals, MC bkgs.
	Data-driven bkg. est.	-	1%	1%	V + jets
	Data-driven bkg. est.	-	-	1%	$t\bar{t}$

Table 1: Overview of systematic uncertainties considered.

Uncertainties	$\delta\kappa_\lambda$ (68% CL)
Stat. only	3.2%
Syst. 1	3.6%
Syst. 2	3.9 %
Syst. 3	5.7 %

Table 2: Expected precision on κ_λ when combining the $b\bar{b}\gamma\gamma$ and $b\bar{b}\ell\ell + E_{\mathrm{T}}^{\mathrm{miss}}$ analyses.

To extract the Higgs self-coupling modifier κ_λ from the di-Higgs events, the dependence of the di-Higgs production cross-section on κ_λ is parameterised as a function of the event rates for signals with $\kappa_\lambda = 1.0, 2.4, 3.0$. All other Higgs couplings are fixed to their SM values, and in particular no κ_λ dependence or uncertainties are assumed on the involved branching ratios. The resulting likelihood scans for the κ_λ parameter are shown in Figure 3a. At 68% confidence level, the expected precision on κ_λ ranges from 3.2% in the case of considering only the statistical uncertainty, to 5.7% for the systematic uncertainty scenario 3, as reported in Table 2. This high precision is fully dominated by the $b\bar{b}\gamma\gamma$ analysis, while the best precision reached by the $b\bar{b}\ell\ell + E_{\mathrm{T}}^{\mathrm{miss}}$ analysis is roughly 20% with statistical uncertainties only. Figure 3b shows as an additional interpretation the simultaneous constraints on κ_λ and the κ_t modifier of the Yukawa coupling between Higgs boson and top quark. Here only statistical uncertainties are considered.

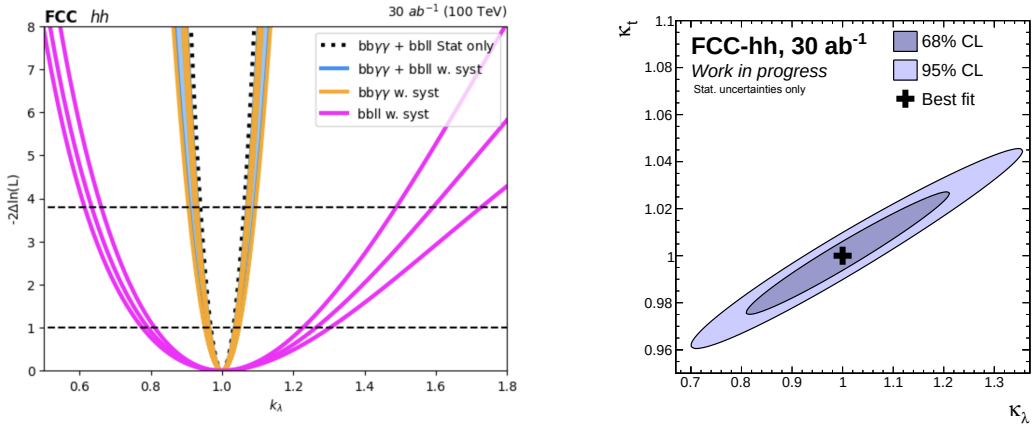

(a) **(b)**

Figure 3: a) Expected likelihood scans as a function of κ_λ for the $b\bar{b}\gamma\gamma$ and $b\bar{b}\ell\ell + E_{\mathrm{T}}^{\mathrm{miss}}$ analyses and their combination. b) Expected likelihood scan as a function of κ_t and κ_λ for the $b\bar{b}\gamma\gamma$ and $b\bar{b}\ell\ell + E_{\mathrm{T}}^{\mathrm{miss}}$ combination.

Acknowledgements

We thank Christophe Grojean for useful discussions, especially on the theory framework, and Michele Selvaggi for providing the DELPHES detector scenario. This work is supported by the Deutsche Forschungsgemeinschaft (DFG, German Research Foundation) under Germany's Excellence Strategy – EXC 2121 „Quantum Universe" – 390833306.

References

[1] ATLAS collaboration, ATL-PHYS-PUB-2022-005.

[2] FCC collaboration, *EPJST* **228** (2019) 755.

[3] M.L. Mangano, G. Ortona and M. Selvaggi, *EPJC* **80** (2020) 1030.

[4] J. De Favereau, C. Delaere, P. Demin, A. Giammanco, V. Lemaitre, A. Mertens et al., *JHEP* **02** (2014) 057.

[5] P. Nason, *JHEP* **11** (2004) 040.

[6] S. Frixione, P. Nason and C. Oleari, *JHEP* **11** (2007) 070.

[7] S. Alioli, P. Nason, C. Oleari and E. Re, *JHEP* **06** (2010) 043.

[8] M. Grazzini, G. Heinrich, S. Jones, S. Kallweit, M. Kerner, J.M. Lindert et al., *JHEP* **05** (2018) 059.

[9] S. Amoroso, P. Azzurri, J. Bendavid, E. Bothmann, D. Britzger, H. Brooks et al., *arXiv* (2020) [2003.01700].

[10] J. Alwall, R. Frederix, S. Frixione, V. Hirschi, F. Maltoni, O. Mattelaer et al., *JHEP* **07** (2014) 079.

[11] R. Frederix, S. Frixione, V. Hirschi, D. Pagani, H.-S. Shao and M. Zaro, *JHEP* **07** (2018) 185.

[12] T. Sjöstrand, S. Mrenna and P. Skands, *Computer Physics Communications* **178** (2008) 852.

[13] P. Fernandez Declara et al., *PoS* **EPS-HEP2021** (2022) 844.

[14] "*EDM4hep data model*." https://edm4hep.web.cern.ch/.

[15] "*FCCAnalyses framework*." https://github.com/HEP-FCC/FCCAnalyses.

[16] A. Gulli and S. Pal, *Deep learning with Keras*, Packt Publishing Ltd (2017).

[17] M. Abadi et al., *arXiv* (2016) [1603.04467].

[18] ATLAS Collaboration, *Physics Letters B* **761** (2016) 350.

[19] C.G. Lester, *JHEP* **05** (2011) 076.